This article has been published in: Clinical Oral Investigations. 2018 Feb 5. doi: 10.1007/s00784-018-2372-7.

Authors:

Raquel Osorio[1].

Manuel Toledano-Osorio [1].

Estrella Osorio[1].

Fátima S. Aguilera[1].

Sussette Padilla-Mondéjar [2].

Manuel Toledano[1].

Title: Zinc and silica are active components to efficiently treat *in vitro* simulated eroded dentin.

Affiliations and addresses:

1. Dental School. University of Granada. Colegio Máximo, Campus de Cartuja s/n. 18071 Granada, Spain. Research Institute IBS.

2. Azurebio S.L. Research and Development Department. Ronda de Pte. Tres Cantos. Madrid. Spain.

Corresponding author:

Raquel Osorio

Dental School, University of Granada.

Colegio Maximo, Campus de Cartuja s/n 18071 Granada, Spain.

Phone: +34-958243793; Fax: +34-958240908.

E-mail: rosorio@ugr.es

ACKNOWLEDGEMENTS: Projects RTC-2014-1731-1 and MAT2014-52036-P supported by the Ministry of Economy and Competitiveness and European Regional Development Fund.

Abstract

Objectives: Biomaterials for treating dentin hypersensitivity and dentin wear were evaluated, to efficiently occlude the dentinal tubules and to increase dentin resistance to abrasion. Materials and Methods: 24 dentin surfaces were treated with EDTA to expose dentinal tubules, and were: 1) non-brushed, 2) brushed with distilled water, or with pastes containing 3) Monetite, 4) Brushite, 5) Zn-Monetite, 6) Zn-Brushite, 7) Silica-Brushite and 8) NovaMin®. Topography, nanomechanical and chemical analysis were assessed on dentin surfaces (n=3) after artificial saliva immersion for 24 h, and after citric acid challenge. 21 further dentin specimens were created to evaluate dentin permeability after brushing, saliva storage and acid application (n=3). ANOVA, Student-Newman-Keuls ($p<0.05$) and Student *t*-test ($p<0.001$) were used. Results: Particles containing major proportion of silica attained intratubular occlusion by carbonate crystals (Raman carbonate peak heights: 15.17 and 19.24 au; complex modulus: 110 and 140 GPa, at intratubular dentin). When brushing with pastes containing higher proportion of silica or zinc, phosphate calcium compounds were encountered into tubules and over dentin surfaces (Raman intratubular phosphate peak heights: 49 to 70 au, and at the intertubular dentin: 78 to 92). The formed carbonated apatite and calcium phosphate layer were resistant to citric acid application. Zinc compounds drastically increased tubule occlusion, decreased dentin permeability (up to 30%) and augmented mechanical properties at the intertubular dentin (90-130 GPa), it was maintained after acid challenging. Conclusions: Zinc-containing pastes occluded dentinal tubules and improved dentin mechanical properties. Clinical Relevance: Using zinc as an active component to treat eroded dentin is encouraged.

Key words: zinc, silica, dentin, mechanical properties, Raman.

Introduction

Tooth tissue wear due to abrasion, attrition, abfraction and erosion has become a concern, as the population ages [1]. Loss of enamel, dental cementum or surrounding soft tissue will lead to exposed dentin. Exposed dentin is subjected to physical and chemical challenges and it frequently produces caries and hypersensitivity [2].

A biomaterial for treating dentin hypersensitivity is desired, not only to efficiently occlude the dentinal tubules but also to maintain the effect at the long-term, especially when confronted with dietary acid and mechanical challenges [3]. Previously reported treatments range from the use of products containing active ingredients that either desensitize the nerve tissue at the base of the dentin tubule (e.g. potassium salts) [2] or by encouraging the promotion of dentin tubule occlusion (e.g. fluoride and other materials able to liberate calcium and phosphate into the tubules)[1,4]. The hydrodynamic fluid movement is the principal mechanism of action for the manifestation of dentin hypersensitivity. Substances that cause a decrease in the dentinal fluid conductance, by occluding the tubules, will reduce dentin hypersensitivity and tooth decay [5].

The use of bioactive materials (able to induce the formation a calcium phosphate layer when immersed in simulated body fluid solution) has also been proposed [4,6]. Recently, a bioactive glass (NovaMin®, developed by NovaMin Technology Inc., Alachua, FL, USA) based on the original 45S5 Bioglass® (US Biomaterials Corp., Jacksonville, FL, USA) composition has been incorporated as a remineralizing agent in dentifrice formulations. The 45S5 are bioactive glass particles that are supposed to trigger an ionic reaction. When the glass particles contact saliva and water, the glass releases calcium and phosphate ions that form a calcium phosphate layer [4]. Supposedly, it is then converted into hydroxyapatite (HAp), which creates a physical barrier over the tubules. On the other side, it has also been described, that the application of these particles may act as abrasive, producing a smear layer able to close the tubules [4]. Durability of this smear layered tubule occlusion is questioned [4,6,7,8]. This formed smear layer is generally inert [9], and confers a short term level of tubule occlusion [1].

Most of the previously published studies [4,7,9,10,11,12] evaluate the efficacy of these remineralizing products by examining the degree of tubule occlusion conferred by the desensitizing materials. These reports are far to elucidate the quality of the formed mineralized layer and to distinguish it from a weak smear layer due to dentin abrasion.

Therefore, nanomechanical and chemical characterization of this new formed outer layer is proposed in the present investigation.

New experimental crystalline and highly porous particles of calcium phosphate, zinc and a calcium-free silicon compound are proposed. Zinc has been included as it has been shown to have high affinity to dentin, similarly to other metals used for treating hypersensitivity such as strontium or tin [1]. Zinc is an antibacterial [7] and it is also a matrix metalloproteinases inhibitor [13,14]. Recent scientific findings demonstrate that inhibition of metalloproteinases is crucial to act against the progression of dentin erosion [15,16].

The null hypothesis to be tested is that treating dentin with different bioactive particles does not modify the surface topography, dentin permeability, chemical and nanomechanical properties of the treated dentin surfaces.

Materials and Methods

Bioactive materials preparation: Composition of experimental particles is displayed in Table 1. Calcium phosphates are selected from dicalcium phosphate anhydrous [monetite, $Ca_{1-x}M_xHPO_4$], dicalcium phosphate dihydrate [Brushite $Ca_{1-x}M_xHPO_4 \cdot 2H_2O$], or HAp [$Ca_{10-x}M_x(PO_4)_6(OH)_2$], where $0 \leq x \leq 0.1$ and where M is a divalent metallic ion (zinc). Incorporation of zinc as partial substitutions of Ca^{++} in the calcium phosphates provides the means for zinc release to contribute to dentin remineralization. Therefore, in some groups Ca^{++} is partially substituted by Zn [Zn-monetite, $Ca_{1-x}Zn_xHPO_4$], dicalcium phosphate dehydrate where Ca^{++} is partially substituted by Zn [Zn-Brushite $Ca_{1-x}Zn_xHPO_4 \cdot 2H_2O$]. Calcium-free silicon compound (silica gel) is also present in materials composition. Particles are produced by acid-base hydraulic reactions as reviewed by Chow [17]. Temperature and humidity conditions may favor the formation of crystals of dehydrated dicalcium phosphate [monetite, $CaHPO_4$], hydrated dicalcium phosphate [Brushite $CaHPO_4 \cdot 2H_2O$] and/or HAp [$Ca_{10}(PO_4)_6(OH)_2$]. Particles with an average particle size less than 20 μm were produced by grinding procedures after fabrication. Field emission scanning electron microscopy (FESEM) (GEMINI, Carl Zeiss SMT, Germany) pictures of produced particles are presented in figure 1.

A flow chart representing the study design and employed methods is provided in Figure 2.

Dentin specimens preparation for surface analysis: Twenty four non-carious human third molars were obtained with informed consent from donors (18 to 25 yr of age), under a protocol approved by the Institution review board (#892/2014). The teeth were stored in 0.01% (w/v) thymol solution at 4ºC. Twenty four dentin discs (0.75mm ± 0.08mm thick) were sectioned (Isomet 4000, Buehler, Lake Bluff, IL, USA) from the mid-coronal portion of the crown. One slice was obtained from each tooth. The surfaces were polished through SiC abrasive papers from 800 up to 4000 grit followed by final polishing steps performed using diamond pastes through 1 μm down to 0.25 μm (Struers LaboPol-4; Struers GmbH, Hannover, Germany). Tubules were exposed by dipping the dentin discs into 0.5 M Ethylenediaminetetraacetic acid (EDTA) solution (pH 7.4) for 2 min [6]. Mix of experimental powders (table 1) was performed with deionized water (at a concentration of 1 g/ml) for 30 s, and EDTA-treated specimens were brushed with the pastes, containing the experimental particles: monetite (M); Zn-monetite (Zn-M); brushite (B); Zn-brushite (Zn-B); Silica gel and brushite (SGB); and NovaMin® (NV). A control group brushed with distilled water (DW) and discs of EDTA-treated dentin specimens were also analyzed. For the tooth brushing procedure, an electric tooth-brush (Oral-B Vitality Precision Clean, P&G Barcelona, Spain) was used for 2 min. The brush was stabilized with the aid of a micro-manipulator (World Precision Instruments Ltd., London, UK) and a force of 70 g was applied to ensure for a constant pressure during the procedure. Each group had an assigned soft brush head. Then, specimens were rinsed with deionized water for 60 s. and immersed in artificial saliva [50 mM/l HEPES, 5 mM/l $CaCl_2.2H_2O$, 0.001 mM/l $ZnCl_2$, 150 mM/l NaCl and 100 U/ml penicillin, 1000 μg/ml streptomycin (pH 7.2)] for 24 h. Dentin discs were then fractured in two halves; half of each dentin disc was directly evaluated for topography, nanomechanical properties and chemical surface analysis (a slightly polishing using diamond pastes 0.25 μm was performed before testing the surfaces). The other halves were analyzed after being submitted to an acid challenge. They were soaked in a 6 wt% citric acid solution (pH = 1.5) for 1 min, then rinsed with deionized water [11].

Atomic force microscopy (AFM) surface characterization: The imaging process was undertaken in the tapping mode, using an AFM (Nanoscope V, Digital Instruments, Veeco Metrology group, Santa Barbara, CA, USA) with a calibrated vertical-engaged piezo-scanner. A 10-nm-radius silicon nitride tip was attached to the end of an oscillating cantilever that came into intermittent contact with the surface at the lowest point of the

oscillation. Changes in vertical position of the AFM tip at resonance frequencies near 330 kHz provided the height of the images registered as bright and dark regions. Measurements were performed in a wet cell, under hydrated conditions. Three 15 x 15 μm digital images were recorded from each surface, with a slow scan rate (0.1 Hz). For each image, five randomized boxes (5 μm × 5 μm) were created and mean surface nanoroughness in each box was recorded (SRa, in nanometers) and considered as a statistical unit.

Nanomechanical properties assessment: Nanomechanical properties were assessed by means of a Hysitron Ti Premier nanoindenter (Hysitron, Inc., Minneapolis, MN), a commercial nano-DMA package. The nanoindenter tip was calibrated against a fused quartz sample using a quasistatic force setpoint of 2 μN to maintain contact between the tip and the sample surface. A dynamic (oscillatory) force of 2 μN was superimposed on the quasistatic signal at a frequency of 200 Hz. Based on a calibration-reduced modulus value of 69.6 GPa for the fused quartz, the best-fit spherical radius approximation for tip was found to be 85 nm, for the selected nano-DMA scanning parameters. Modulus mapping of our samples was conducted by imposing a quasistatic force setpoint, F_q=2 μN, to which we superimposed a sinusoidal force of amplitude F_A=0.10 μN and frequency f=100 Hz. The resulting displacement (deformation) at the site of indentation was monitored as a function of time. Specimens were scanned under a hydrated condition. Three randomized regions approximately 15×15 μm in size were created at each surface using a scanning frequency of 0.2 Hz. Complex modulus data were collected from each of these scanned regions and a mean was calculated for each scanned surface, it was considered a statistical unit. Under steady conditions (application of a quasistatic force) the indentation modulus of the tested sample, E, can be obtained by application of different models that relate the indentation force, F, and depth, D [18].

Surfaces Raman Analysis: A dispersive Raman spectrometer/microscope (Horiba Scientific Xplora, Villeneuve d´Ascq, France) was also used to analyze treated dentin surfaces. A 785-nm diode laser through a X100/0.90 NA air objective was employed. Raman signal was acquired using a 600-lines/mm grafting centered between 900 and 1,800 cm^{-1}.Chemical mapping of the interfaces were performed. For each specimen two areas 15μm x 15μm area of the interfaces at different sites were mapped using 2 μm spacing at X axis and 1 μm at Y axis. At this point, the mineral component of dentin was assessed as follows: 1) the mineral matrix ratio (MMR: the relative mineral content, or the degree of demineralization as a function of spatial position, which was determined

from the ratios of the relative integrated intensities of spectral features associated with phosphate (P–O symmetric stretch: ν_1-961 cm^{-1}) or carbonate (1070 cm^{-1}) and collagen (CH_2 deformation: 1454cm^{-1}); 2) the relative presence of mineral (RPM: the phosphate peak height (ν_1-961 cm^{-1}) and the carbonate peak height (1070 cm^{-1}); and 3) the degree of crystallinity (FWMH: the full width at half maximum of the phosphate (ν_1-961 cm^{-1}) and carbonate (1070 cm^{-1}) bands, as it expresses the crystallographic or relative atomic order; the narrower the spectral peak width, the higher the degree of mineral crystallinity.

Dentin Permeability Evaluation: Twenty one non-carious human third molars were obtained and stored following the same conditions explained above. Mid-coronal dentin blocks were created. Occlusal enamel was removed using a slow-speed, water-cooled diamond saw, and in this case a second parallel cut was performed 1.5 mm beneath the cementum-enamel enamel junction in order to remove the roots. Removal of pulp tissue was performed, taking care not to touch the predentin surface and the inner part of the pulpal chamber. Flat dentin surfaces were polished and smear layer on both sides of the dentin blocks was removed by immersion in 0.5 M EDTA solution (pH 7.4) for 2 minutes. Dentin specimens were bonded to Plexiglas blocks penetrated with an 18-gauge stainless steel tube. Specimens were connected to a hydraulic pressure device with a liquid flow sensor (ASL 1600, Sensirion, Staefa, Switzerland). A constant hydraulic pressure of 6.9 kPa was applied [12]. The measurement of the fluid volume through the sensor was performed. The highest hydraulic conductance for each specimen after EDTA treatment was recorded (P_{max}). Dentin permeability was calculated after pastes or distilled water application and artificial saliva storage for 24 h and additional measurements were performed after applying citric acid to each dentin surface, in the same conditions exposed above. Three specimens were tested per group. Five fluid volume readings were recorded every 3 min during 15 min. The permeability of each specimen and condition was expressed as a percentage of the fluid flow through the EDTA-treated dentin disc of the same specimen (P_{max}), the percentage of permeability reduction was calculated [12].

Statistical analysis: After testing data normal distribution by Kolmogorov-Smirnov, ANOVA and Student-Newman-Keuls multiple comparisons tests were performed to compare between experimental groups ($p<0.05$). Student *t* tests were also used to ascertain differences between saliva stored vs. acid challenged specimens within the same experimental group ($p<0.001$). The IBM SPSS Statistics 20 computer software was employed.

Results

Atomic force microscopy (AFM) surface characterization: Representative AFM images of treated dentin surfaces are presented in Figure 3; morphological differences may be appreciated. At the EDTA-treated dentin specimens, collagen fibres were evidenced but after saliva immersion, all groups presented tubular occlusion. The surfaces appeared covered by a continuous and homogeneous layer, not being possible to observe collagen fibrils or dentinal tubules, except for those dentin surfaces that were brushed with distilled water or with Monetite particles. In these groups, tubules were evident and not completely closed. Mean nanoroughness values measured at intertubular dentin of these surfaces are shown in table 2. A significant decrease in nanoroughness at the intertubular dentin was observed in all groups, after brushing and artificial saliva storage. When the citric acid challenge was applied, roughness at the intertubular dentin follows the following trend SGB<Zn-M=B<M=Zn-B=NV<DW. After the citric acid challenging, dentin tubules were occluded in all groups, except for those specimens brushed with distilled water, brushite or monetite particles.

Nanomechanical properties assessment: Relevant complex modulus mapping of dentin specimens brushed with the different experimental pastes are presented in Figure 4. Means and standard deviations are displayed in Table 2. After 24 h storage in artificial saliva, those dentin specimens brushed with silica or zinc based compounds (Zn-B, Zn-M, SGB, and NV) attained the highest mechanical properties at intertubular, peritubular and intratubular dentin. Complex modulus values follow the trend: DW<M=B<Zn-B=SGB<NV<Zn-M. After the citric acid challenging, specimens brushed with Zn-M attained the highest complex modulus values. Complex modulus values are ordered as follows DW<B<M<Zn-B=NV<SGB<Zn-M.

Surfaces Raman Analysis: Representative phosphate and carbonate peak height mapping performed on the different dentin specimens is provided in Figure 5. The relative presence of mineral and degree of crystallinity values obtained for the different experimental groups are displayed in Table 3. After 24 h of saliva storage, the relative presence of phosphate [961 cm^{-1}] based mineral was higher for dentin specimens brushed with Zn-B or NV at intertubular and intratubular dentin. Carbonate [at 1070 cm^{-1}] peak height was also higher for these experimental groups. After citric acid application, the major presence of mineral related to 961 cm^{-1} phosphate and to 1070 cm^{-1} carbonate peaks were attained at the intertubular dentin regions for the experimental groups Zn-B, Zn-M, NV

and SGB. At the intratubular dentin, the highest phosphate and carbonate related peaks were obtained for the groups NV and SGB.

Dentin Permeability Evaluation: Mean dentin permeability values measured at treated dentin blocks are shown in table 4. A significant decrease in permeability was produced after application of those particles containing zinc or silica, following the same trend before and after acid application: NV=SGB=Zn-B=Zn-M<B=M=DW. Acid application did not alter permeability except in the groups of DW, M and B, in these groups permeability was augmented.

Discussion

This study tried to gain insights into the role of experimental particles leading to remineralization and mechanical recovery of eroded and demineralized dentin. To detect changes in the chemistry and structure of experimental samples, a combination of different analytical techniques was employed. AFM assessed changes in morphology and tubule occlusion, Nano-DMA ascertained for surface mechanical properties and Raman spectroscopy probed atomic interactions in formed compounds. Dentin permeability was also assessed in order to analyse effective tubule occlusion.

After brushing and artificial saliva storage for 24 h, all groups presented tubular occlusion except those dentin surfaces that were brushed with distilled water or monetite pastes (Figure 3). Particles in paste formulations act as abrasives, occluding dentin tubules [4,9]. Nevertheless, they may be inert conferring a short term level of occlusion or bioactive being able to form more stable mineral deposits. Smear layer creation by bristles and abrasives have been shown to decrease dentin permeability up to 40% due to tubule occlusion [6]. In the present study distilled water, brushite and monetite pastes produced low reduction of dentin permeability (fluid flow values ranged from 50 to 65%)(table 4), which may indicate the existence of inert smear layer formation. Saliva can solubilize ions from particles adhering to teeth. Besides, mineral salts from saliva may also facilitate precipitates on the dentin surface, which leads to some degree of dentin tubule occlusion [12,19]. To permit for AFM and nanohardness analyses, the dentin samples needs to be slightly polished before examination. This polishing will remove slight smear layers. In the groups of distilled water and monetite more delicate mineral deposits were formed and could not even resist the polishing action. Therefore, the formed smear layer was partially eliminated. The formation of distinct dentin smear layers when employing monetite or brushite pastes may be explained: i) by differences in hardness of these

mineral particles. Mosh hardness for monetite is 3.5 [20] and for brushite is 2.5 [21], whereas dentin has approximately a value of 3 [22]; and ii) by differences in particles bioactivity, as brushite is bioactive and will be able to form mineral deposits. In fact, it is an acidic calcium phosphate that will form HAp when pH value is around 7 [23].

In many other cases, it has been previously observed that despite the high amount of deposits encountered on the surfaces and in the tubules, the tubule occlusion may be easily washed away [12,24], as it occurred with monetite paste (Figure 3). The lowest complex modulus reported for surfaces brushed with distilled water and monetite confirm the formation of this smear layer (Table 2, Figure 4). Tested experimental pastes have distinct active ingredients, which conferred the ability to permanently occlude dentin tubules. To ascertain between the presented pastes, which one can efficiently occlude the dentinal tubules and obtain acid-resistant stability, citric acid was further applied. Citric acid is widely used in *in vitro* studies to simulate the oral environment and is able to test the resistance of smear layers created by dentin desensitizers [12].

After challenging the dentin surfaces with citric acid, tubules remained occluded in all specimens except for those brushed with distilled water, monetite and brushite pastes (Figure 3). Dentin permeability values of these groups significantly increased from (64, 59 and 55 up to 98, 87 and 86% respectively) (table 4). Thus, the formed permanent tubule occlusion in the other groups can be attributed purely to the effect of zinc or higher silica contain in pastes composition.

Zinc has been shown to facilitate dentinal tubules occlusion by crystals precipitation, and these new formed crystals were not easily dissolved after acids application [26]. The precipitation of a calcium phosphate compound has also been observed when testing bioactivity of other zinc containing biomaterials. Hence, the formed HAp in these conditions was found to be more resistant to solubility, being crystal solubility directly related to zinc concentration in these biomaterials [27]. It may explain the acid-resistant occlusion of dentinal tubules, at those specimens brushed with Zn-containing compounds.

NovaMin® reacts in aqueous environments, and releases calcium, sodium, and phosphate. It seems that sodium ions are important as they begin to exchange with hydrogen cations, which lately permit calcium and phosphate releasing from the filler particle structure [28]. Finally, they are able to form a calcium phosphate layer onto the dentin surfaces and into the tubules [4,28]. Moreover, sodium phosphate salts in solution also facilitates HAp formation [29]. These salts help to control the high alkalinising potential of HAp formation, permitting prolonged phosphatase alkaline activity.

NovaMin® action is also enhanced by silicates, which are able to promote HAp deposits formation, improving calcium phosphate compounds bioactivity [30,31]. Same effect may be attributed to silica gel-brushite particles employed in the present study that accounted together with NovaMin®, Zn-brushite and Zn-monetite for an acid-resistant tubule occlusion (Table 2, Figures 3 and 4).

At the intertubular dentin, specimens treated with NovaMin®, Zn-monetite, Zn-brushite or silica gel-brushite attained higher relative content of minerals (carbonate and phosphate peak intensities) compared to dentin surfaces treated with the other pastes (Table 3, Figure 5). When considering intratubular dentin, NovaMin® and silica gel-brushite pastes attained the highest mineralization, even after citric acid challenge. It is worth mentioning, the relative high level of carbonate presence at intratubular dentin when NovaMin® or silica-gel pastes were employed (Table 3, Figure 5). It has been previously reported that introduction of calcium-sodium-phosphosilicate, into the oral environment, results in the formation of carbonated HAp [4,7,28].

Concerns have been previously expressed over the durability of carbonated HAp, as it may dissolve readily when teeth are exposed to acidic conditions [7]. In the present study, after Raman analysis, it is shown that the relative presence of mineral measured at the carbonate peak did not decrease after citric acid challenging when NovaMin® or silica gel-brushite pastes are employed, neither at the intratubular or the intertubular dentin (Table 3, Figure 5).

However, restoring of dentin does not only relate to tubule occlusion but also to an improvement on mechanical properties and mineralization at the intertubular dentin, that will impair the progression of eroded lesions. The highest mechanical properties at the intertubular and intratubular dentin were obtained for Zn-monetite followed by silica gel-brushite. Slightly lower values were obtained for Zn-brushite and NovaMin® pastes, without significant differences between them (Table 2, Figure 4). Biological apatite is calcium deficient and contains substantial amounts of carbonate. Carbonated apatite is a precursor of HAp, but when it is precipitated in the presence of zinc an exchange between Zn^{2+} and Ca^{2+} occurs *in vitro,* forming a substituted apatite compound [32]. An isomorphous substitution can be obtained when Ca^{2+} is replaced by Zn^{2+} into HAp. Scholzite crystals -$CaZn_2(PO_4)_2 \cdot 2H_2O$- formation during dentin remineralization have previously been described [33]. A higher nanohardness and lower solubility was found in this zinc-substituted mineralized layer [33,34]. Zinc has also been shown to facilitate hard tissue remineralization processes [35].

Both surface mechanical properties and nanoroughness have been previously considered as indirect measurements of dentin remineralization [2]. Attained measurements after citric acid with both analyses were consistent in the present study, being the groups treated with Zinc-monetite and Silica gel with brushite those with the highest complex modulus values (Table 2).

A difficult equilibrium between abrasivity and bioactivity of particles should be obtained. NovaMin® is an amorphous glass, and has a Mohs hardness of 6. It is a hard particle. NovaMin® particles have a hardness value high above the hardness value of dentin and also to that of enamel. In terms of abrasive wear during tooth brushing, it would be desirable to have a glass that is lower to the hardness values of natural enamel in order to minimize the loss of enamel [36]. The experimental particles in the present study, which were obtained by acid-base reactions, result in highly porous materials. It produces a high contact surface area and lower mechanical properties of the particles, contributing towards an increased solubility, and a lower abrasivity [17]. It is in contrast with fully amorphous nature of bioglasses obtained by sol-gel or melting processes that lead to slowly soluble and low-porosity materials with higher abrasibity values.

Zinc-monetita, Zinc-brushite and Silica-gel-brushite particles produced by acid-base hydraulic reaction were able to block dentinal tubules. Particularly, Zinc-brushite improved mechanical properties of intertubular dentin, which is desirable to clinically reduce and prevent the progression of non-carious cervical lesions. A metalloproteinases inhibition effect of zinc-containing particles [13], at this specific dentin site, may also help to stop the progression of these lesions.

It should be taken into account that it has not been previously proven that a single acid contact may be clinically relevant to evaluate the tubules occlusion efficacy, when testing active components to treat non-carious cervical lesions. It just serves as a possible tool to closely resemble the clinical scenario. Therefore, attained results encourage us to proceed with controlled clinical studies in order to really prove for the efficacy of the presented materials [37]. Moreover, a detailed study on the presented particles morphology, size distribution, solubility, dentin abrasion through RDA-values and minerals gain on dentin by transverse microradiography [38] also deserves further research. The absence of these tests should be considered as a limitation of the present study.

COMPLIANCE WITH ETHICAL STANDARDS:

Conflicts of Interest: Raquel Osorio declares that she has no conflict of interest. Estrella Osorio declares that he has no conflict of interest. Fátima S. Aguilera declares that she has no conflict of interest. Sussette Padilla-Mondéjar declares that she has no conflict of interest. Manuel Toledano declares that he has no conflict of interest. Manuel Toledano-Osorio declares that he has no conflict of interest.

Funding: Projects MAT2014-52036-P and RTC-2014-1731-1, both supported by the Ministry of Economy and Competitiveness and European Regional Development Fund.

Ethical Approval: The present protocol was approved by the Ethical Institution Review Board (#892/2014). All procedures performed in the present study, involving human participants, were in accordance with the ethical standards of the institutional and/or national research committee and with the 1964 Helsinki declaration and its later amendments or comparable ethical standards. This article does not contain any studies with animals performed by any of the authors.

Informed consent: Informed consent was obtained from all individual participants included in the study.

REFERENCES

1. Pashley DH (1986) Dentin permeability, dentin sensitivity, and treatment through tubule occlusion. J Endod 12:465-474. doi: 10.1016/S0099-2399(86)80201-1

2. Saeki K, Marshall GW, Gansky SA, Parkinson CR, Marshall SJ (2016) Strontium effects on root dentin tubule occlusion and nanomechanical properties. Dent Mat 32:240-251. doi: 10.1016/j.dental.2015.11.020

3. Zhou J, Chiba A, Scheffel DLS, Hebling J, Agee K, Niu L-na, et al (2016) Effects of a Dicalcium and Tetracalcium Phosphate-Based Desensitizer on In Vitro Dentin Permeability. PLoS ONE 11: e0158400. doi:10.1371/journal.pone.0158400

4. Wang Z, Jiang T, Sauro S, Pashley DH, Toledano M, Osorio R, Liang S, Xing W, Sa Y, Wang Y (2011) The dentine remineralization activity of a desensitizing bioactive glass-containing toothpaste: an in vitro study. Austr Dent J 56:372-381. doi: 10.1111/j.1834-7819.2011.01361.x

5. Markowitz K, Pashley DH (2008) Discovering new treatments for sensitive teeth: the long path from biology to therapy. J Oral Rehabil 35:300-315. doi: 10.1111/j.1365-2842.2007.01798.x

6. Wang Z, Sa Y, Sauro S, Chen H, Xing W, Ma X, Jiang T, Wang Y (2010) Effect of desensitising toothpastes on dentinal tubule occlusion: A dentine permeability measurement and SEM in vitro study . J Dent 38:400-410. doi: 10.1016/j.jdent.2010.01.007

7. Lynch E, Brauer DS, Karpukhina N, Gillam DG, Hill RG (2012) Multi-component bioactive glasses of varying fluoride content for treating dentin hypersensitivity. Dent Mat 28:168-178. doi: 10.1016/j.dental.2011.11.021

8. Arnold WH, Gröger CH, Bizhang M, Naumova1 EA (2016) Dentin abrasivity of various desensitizing toothpastes. Head & Face Medicine 2:12-16. doi:10.1186/s13005-016-0113-1

9. Prati C, Venturi L, Valdre` G, Mongiorgi R (2002) Dentin morphology and permeability after brushing with different toothpastes in the presence and absence of smear layer. J Periodontol 73:183-190. doi:10.1902/jop.2002.73.2.183

10. Gandolfi MG, Iacono F, Pirani C, Prati C (2012) The use of calcium-silicate cements to reduce dentine permeability. Arch Oral Biol 57:1054-1061. doi: 10.1016/j.archoralbio.2012.02.024

11. Farooq I, Moheet IA, Al Shwaimi E (2015) In vitro dentin tubule occlusion and remineralization competence of various toothpastes. Arch Oral Biol 60:1246-1253. doi:10.1016/j.archoralbio.2015.05.012

12. Sauro S, Lin CY, Bikker FJ, Cama G, Dubruel P, Soria JM, D'Onofrio A, Gillam D (2016) Di-Calcium Phosphate and Phytosphingosine as an Innovative Acid-Resistant Treatment to Occlude Dentine Tubules. Caries Res 50:303-309. doi:10.1159/000445444

13. Osorio R, Yamauti M, Osorio E, Ruiz-Requena ME, Pashley DH, Tay FR, Toledano M (2011) Zinc reduces collagen degradation in demineralized human dentin explants. J Dent 39:148-153. doi: 10.1016/j.jdent.2010.11.005

14. Toledano M, Yamauti M, Osorio E, Osorio R (2012) Zinc-inhibited MMP-mediated collagen degradation after different dentine demineralization procedures. Caries Res 46:201-207. doi: 10.1159/000337315

15. Kato MT, Leite AL, Hannas AR, Oliveira RC, Pereira JC, Tjäderhane L, et al. (2010) Effect of iron on matrix metalloproteinase inhibition and on the prevention of dentine erosion. Caries Res 44:309-316. doi: 10.1159/000315932

16. Buzalaf MA, Charone S, Tjäderhane L (2015) Role of host-derived proteinases in dentine caries and erosion. Caries Res 49: 30-37. doi: 10.1159/000380885

17. Chow LC (2009) Next generation calcium phosphate-based biomaterials. Dent Mater J 28: 1-10.

18. Han L, Grodzinsky AJ, Ortiz C (2011) Nanomechanics of the cartilage extracellular matrix. Annu Rev Mater Res 41: 133-168. doi:10.1146/annurev-matsci-062910-100431

19. Suge T, Kawasaki A, Ishikawa K, Matsuo T, Ebisu S (2008) Ammonium hexafluorosilicate elicits calcium phosphate precipitation and shows continuous dentin tubule occlusion. Dent Mat 24:192-198.doi:10.1016/j.dental.2007.03.009

20. Catti M, Ferraris G, Filhol A (1977) Hydrogen bonding in the crystalline state. $CaHPO_4$ (monetite), $P\bar{1}$ or $P1$? A novel neutron diffraction study. Acta Cryst B33:1223.

21. Murray JW, Dietrich RV: Brushite and taranakite from Pig Hole Cave, Giles County, Virginia. Am Mineral 1956;41:616.

22. Marshall GW Jr, Marshall SJ, Kinney JH, Balooch MJ (1997) The dentin substrate: structure and properties related to bonding. J Dent 25:441-458. doi:10.1016/S0300-5712(96)00065-6

23. Schwarz ML, Kowarsch M, Rose S, Becker K, Lenz T, Jani L (2009) Effect of surface roughness, porosity, and a resorbable calcium phosphate coating on

osseointegration of titanium in a minipig model. J Biomed Mater Res A 89:667-678. doi: 10.1002/jbm.a.32000

24. Addy M, Mostafa P (1989) Dentine hypersensitivity. II. Effects produced by the uptake in vitro of toothpastes onto dentine. J Oral Rehabil 16:35-48.

25. Chiang YC, Chen HJ, Liu HC, Kang SH, Lee BS, Lin FH, Lin HP, Lin1 CP (2010) A Novel Mesoporous Biomaterial for Treating Dentin Hypersensitivity. J Dent Res 89:236-240. doi: 10.1177/0022034509357148

26. Gu H, Ling J, LeGeros JP, LeGeros RZ (2011) Calcium phosphate-based solutions promote dentin tubule occlusions less susceptible to acid dissolution. Am J Dent 24:169-175.

27. Oudadesse H, Dietrich E, Gal YL, Pellen P, Bureau B, Mostafa AA, Cathelineau G (2011) Apatite forming ability and cytocompatibility of pure and Zn-doped bioactive glasses. Biomed Mater 6:035006. doi: 10.1088/1748-6041/6/3/035006

28. Burwell AK, Litkowski LJ, Greenspan DC (2009) Calcium sodium phosphosilicate (NovaMin): remineralization potential. Adv Dent Res 21:35-39. doi: 10.1177/0895937409335621

29. Fulmer MT, Brown PW (1993) Effects of Na_2HPO_4 and NaH_2PO_4 on hydroxyapatite formation. J Biomed Mater Res 27:1095-1102. doi:10.1002/jbm.820270815

30. Oliveira AL, Malafaya PB, Reis RL (2003) Sodium silicate gel as a precursor for the in vitro nucleation and growth of a bone-like apatite coating in compact and porous polymeric structures. Biomaterials 24:2575-2584. doi:10.1016/S0142-9612(03)00060-7

31. Porter AE, Patel N, Skepper JN, Best SM, Bonfield W (2003) Comparison of in vivo dissolution processes in hydroxyapatite and silicon-substituted hydroxyapatite bioceramics. Biomaterials 24:4609-4620. doi:10.1016/S0142-9612(03)00355-7

32. Mayer I, Apfelbaum F, Featherstone JDB (1994) Zinc ions in synthetic carbonated hydroxyapatites. Archs Oral Biol 39:87-90. doi:10.1016/0003-9969(94)90040-X

33. Osorio R, Osorio E, Cabello I, Toledano M (2014) Zinc induces apatite and scholzite formation during dentin remineralization. Caries Res 48:276-290. doi:10.1159/000356873

34. Vasant SR, Joshi MJ (2011) Synthesis and characterization of pure and zinc doped calcium pyrophosphate dihydrate nanoparticles. Europ Physic J Appl Phy 53: 10601. doi:10.1051/epjap/2010100095

35. Lynch RJ, Churchley D, Butler A, Kearns S, Thomas GV, Badrock TC, Cooper L, Higham SM (2011) Effects of Zinc and Fluoride on the Remineralisation of Artificial

Carious Lesions under Simulated Plaque Fluid Conditions. Caries Res 45:313-322. doi:10.1159/000324804

36. Hill R, Gillam DG (2015) Future strategies for the development of desensitising products. In: Gillam D (ed) Dentine hypersensitivity: advances in diagnosis, management and treatment, Springer Publishers, London, pp 157-180

37. Vano M, Derchi G, Barone A, Pinna R, Usai P, Covani U (2017) Reducing dentine hypersensitivity with nano-hydroxyapatite toothpaste: a double-blind randomized controlled trial. Clin Oral Investig. doi: 10.1007/s00784-017-2113-3

38. Al-Abdi A, Paris S, Schwendicke F (2017) Glass hybrid, but not calcium hydroxide, remineralized artificial residual caries lesions in vitro. Clin Oral Investig 21:389-396. doi: 10.1007/s00784-016-1803-6

Figure 1

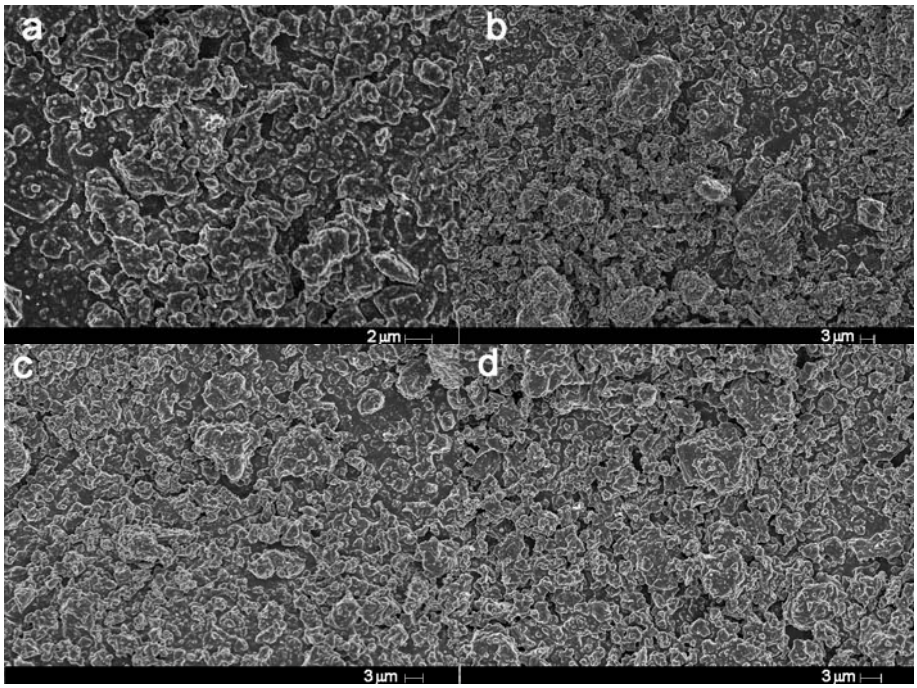

Figure 1 Scanning electron microscopy images of fabricated particles. **a.** Zn-Monetite particles (Zn-M). **b.** Silica gel-brushite particles (SGB). **c.** Monetite particles (M). **d.** Zn-brushite particles (Zn-B)

Figure 2

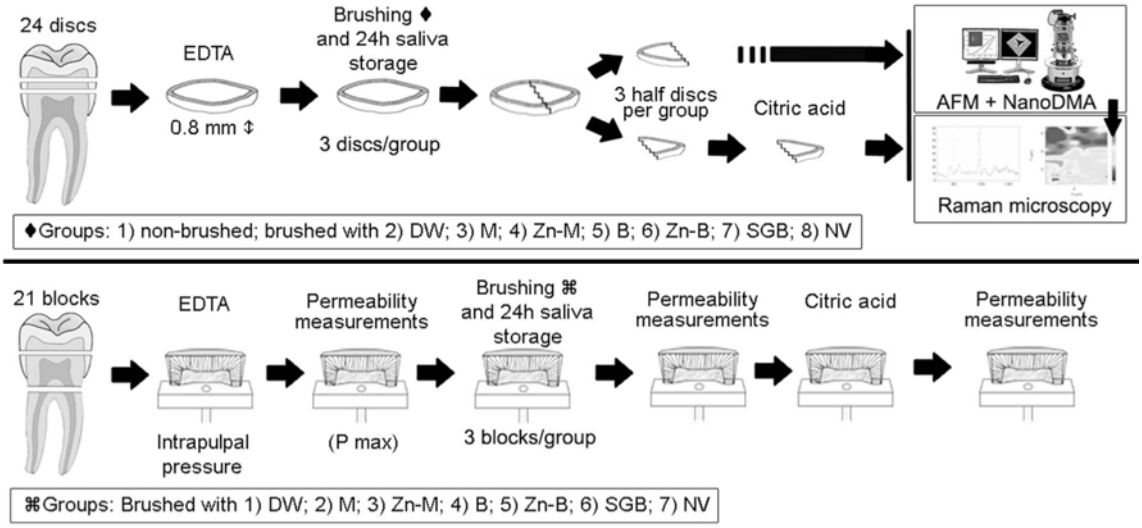

Figure 2 Flow chart represents the study design and the employed methods. DW: distilled water, M: monetite, Zn-M: Zn-monetite, B: brushite, Zn-B: Zn-brushite, SGB: silica gel and brushite, NV: NovaMin®.

Figure 3

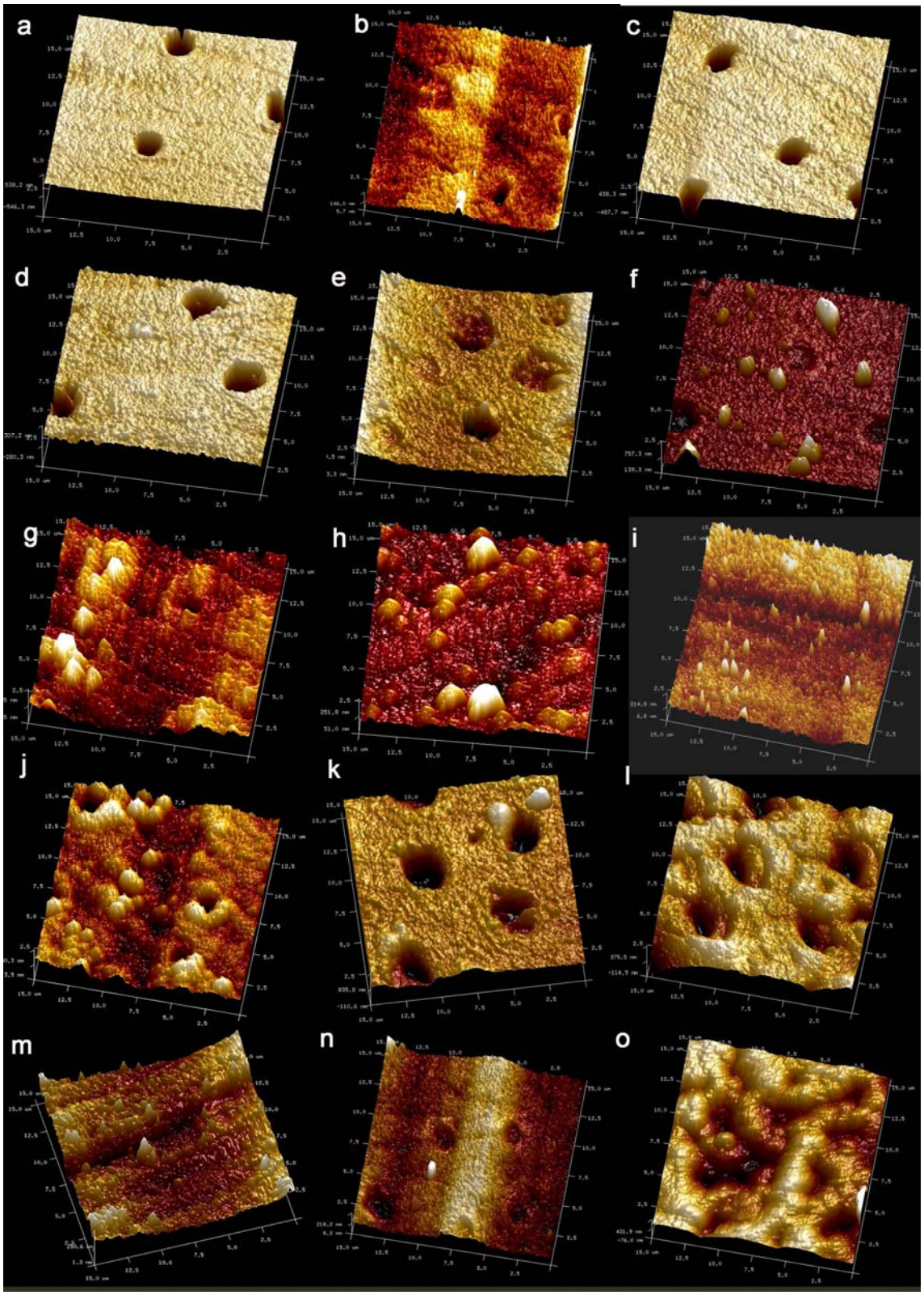

Figure 3 AFM images of the dentin surfaces after application of the different experimental desensitizer pastes and acid challenge. **a.** An EDTA-treated dentin surface in which tubules are open and collagen fibres are evident at the intertubular dentin. **b.** Dentin surface brushed with distilled water after 24 h storage in artificial saliva where collagen fibres appeared covered and tubules may only be partially observed and **c.** Dentin surface brushed with M particles after saliva immersion where tubules are not evident and **d.** after the acid challenge in which enlarged tubules may be encountered at the surface. **e.** Dentin surface brushed with Zn-M particles after saliva storage where tubules are occluded and **f.** after the acid challenge showing closed dentinal tubules and crystal formations protruding at the intertubular dentin. **g.** and **h.** Dentin surfaces brushed with SGB particles after 24 h in artificial saliva and acid challenge respectively, occluded tubules crystal formations are present in both images. **i.** Dentin surfaces brushed with NV particles after 24 h storage in saliva where tubules are occluded and needle shape crystals appeared at the intertubular dentin and **j.** after the acid challenge showing partially occluded tubules with crystals mostly located at the protruding peritubular dentin. **k.** Dentin surfaces brushed with B particles after acid challenge, tubules are partially opened. **l.** Dentin surfaces brushed with Zn-B particles after acid challenge, tubules are closed and intertubular dentin appeared bulging at the surface. **m.** Dentin surfaces brushed with B particles after saliva storage, dentin surface is completely covered and tubules entrances are not observed. **n.** Dentin surfaces brushed with Zn-B particles after saliva storage, dentin tubules are nearly patent but closed. **o.** Dentin surfaces brushed with DW after acid challenge, tubules are opened and collagen fibres are observed at the demineralized intertubular dentin

Figure 4

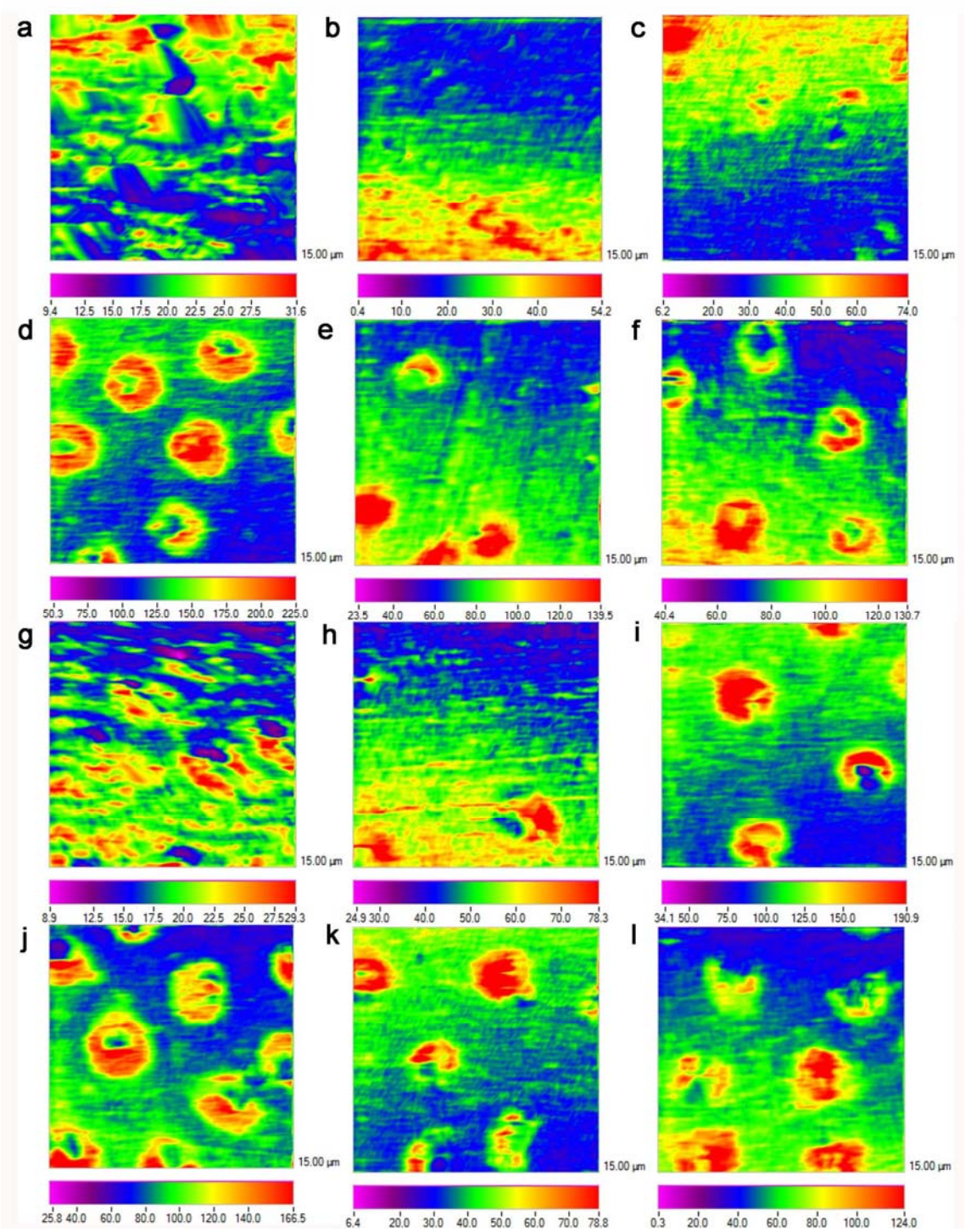

Figure 4 Nano-DMA mapping of the dentin surfaces, after the following treatments: **a.** EDTA, **b.** DW-saliva, **c.** M-saliva, **d.** Zn-M-saliva, **e.** NV-saliva, **f.** GSB-saliva, **g.** DW-acid, **h.** M-acid, **i.** Zn-M-acid, **j.** Z-B-acid, **k.** NV-acid, **l.** GSB-acid. Scale bars are in GPa

Figure 5

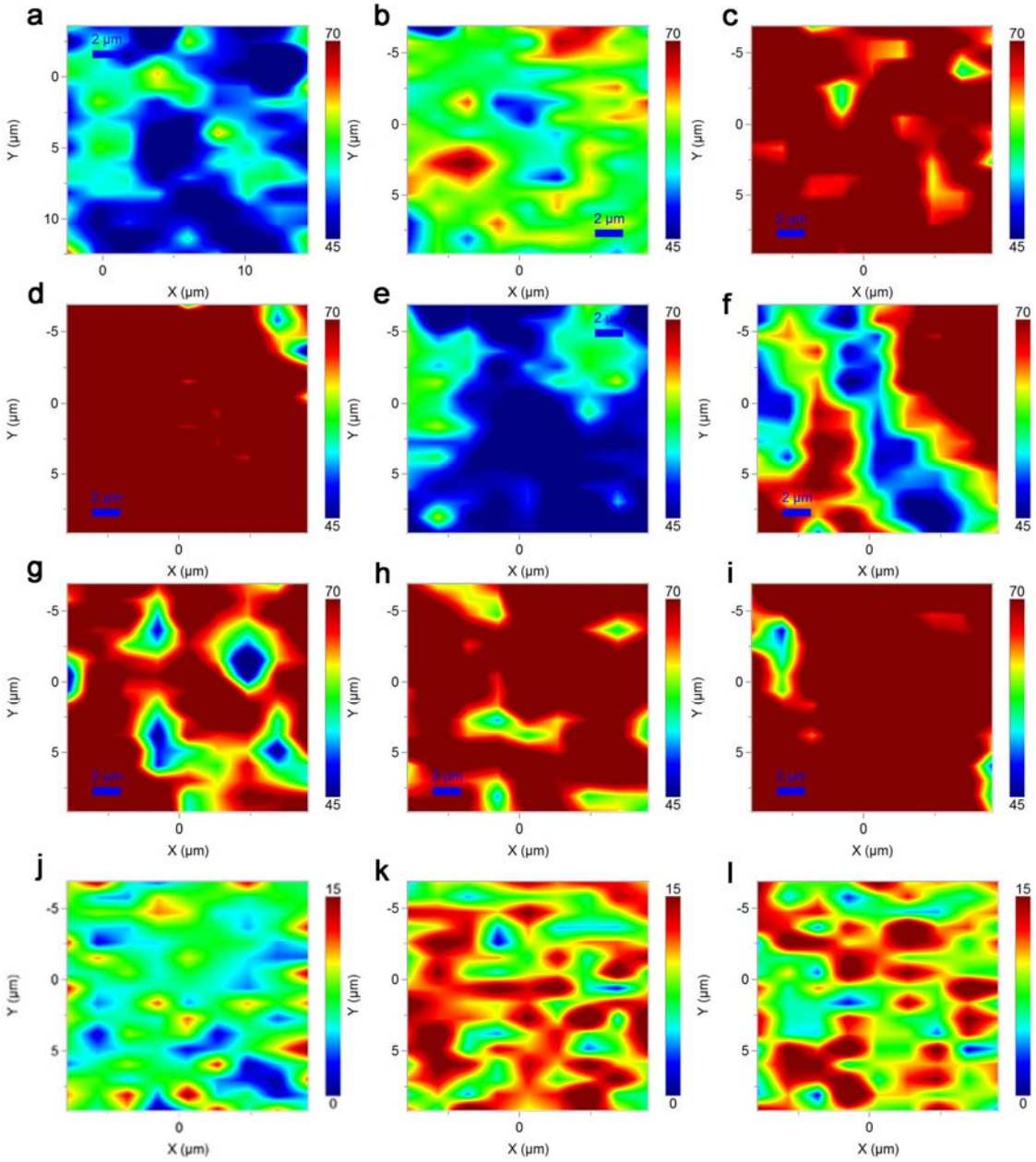

Figure 5 Micro-RAMAN maps of phosphate (**a** to **i**) and carbonate (**j** to **l**) intensities (scale bars in counts) at the dentin surfaces, after the following treatments: **a.** EDTA, **b.** DW-saliva, **c.** Zn-B-saliva, **d.** NV-saliva, **e.** DW-acid, **f.** Zn-B-acid, **g.** Zn-M-acid, **h.** NV-acid, **i.** GSB-acid, **j.** M-acid, **k.** NV-acid, **l.** GSB-acid

Table 1 Chemical composition of experimental particles in the different groups (wt%). **NovaMin®** composition is: 45% SiO, 24.5% Na_2O, 24.5% CaO and 6% P_2O_5.

	M	**B**	**Zn-M**	**Zn-B**	**SGB**
Monetite [$CaHPO_4$]	60	-	-	-	-
Zn-Monetite [$Ca_{1-X}Zn_XHPO_4$]	-	-	60	-	-
Brushite [$CaHPO_4 \cdot 2H_2O$]	-	60	-	-	60
Zn-Brushite [$Ca_{1-x}Zn_xHPO_4 \cdot 2H_2O$]	-	-	-	60	-
Hydroxyapatite [$Ca_{10}(PO_4)_6(OH)_2$]	20	20	20	20	-
Amorphous calcium phosphate [$Ca_xH_y(PO_4)_z \cdot nH_2O$]	10	10	10	10	10
Silica Gel [$SiO_2.H_2O]_n$	10	10	10	10	30

Table 2 Means and standard deviations (SD) of complex modulus of dentin and intertubular dentin nanoroughness after the different treatments. Groups with distinct letters within each dentin type are significantly different after Student-Newman-Keuls multiple comparisons ($p<0.05$). * indicates statistical significance between mean complex modulus of dentin before and after acid challenge within the same experimental group after Student *t* tests ($p<0.001$). **XX**: Values were not calculated as it was not possible to distinguish dentinal tubules at the images.

		Complex Modulus (GPa) Mean (SD)			Intertubular Nanoroughness (SRa) Mean (SD)
		Intertubular	Peritubular	Intratubular	
EDTA		26.88 (2.54)a	21.53 (2.03)a	14.30 (0.56)a	37.60 (6.5)d
After saliva storage	DW	47.38 (10.51)c*	XX	XX	16.69 (1.72)c*
	M	43.66 (6.47)bc*	49.84 (9.47)b*	28.33 (3.73)ab*	18.11 (2.13)c
	Zn-M	130.84 (15.38)f*	145.91 (6.51)g	216.41 (27.20)e	15.73 (2.46)bc*
	B	35.30 (5.75)ab	81.68 (5.83)c*	45.52 (3.20)b*	15.34 (2.83)bc*
	Zn-B	89.73 (11.99)e*	118.97 (8.37)e*	106.04 (23.74)c	12.58 (4.38)b*
	SGB	82.73 (11.44)de*	135.31 (7.31)f*	88.47 (15.68)c*	6.02 (0.98)a*
	NV	75.68 (6.13)d*	103.55 (2.42)d*	175.14 (38.41)d*	14.96 (1.44)bc*
	ANOVA	P<0.001	P<0.001	P<0.001	P<0.001

		Complex Modulus (GPa) Mean (SD)			Intertubular Nanoroughness (SRa) Mean (SD)
		Intertubular	Peritubular	Intratubular	
EDTA		26.88 (2.54) b	21.53 (2.03)a	14.30 (0.56)a	37.60 (6.5)e
After citric acid	DW	19.23 (2.11) a*	27.66 (2.65)b	12.58 (0.64)a	24.72 (4.22)d*
	M	53.40 (1.93) d*	64.54 (2.88)d*	88.44 (15.86)c*	17.31 (1.93)c
	Zn-M	102.16 (6.63) f*	145.23 (14.02)f	233.20 (17.80)f	12.57 (1.62)b*
	B	36.37 (6.72) c	52.25 (4.60)c*	65.73 (4.38)b*	13.40 (1.44)b*
	Zn-B	58.43 (5.09) e*	60.47 (3.38)d*	109.48 (17.56)d	17.25 (2.25)c*
	SGB	53.44 (3.99) d*	79.90 (5.99)e*	140.12 (13.37)e*	9.29 (1.10)a*
	NV	34.71 (3.30) c*	61.14 (3.20)d*	109.71 (19.99)d*	17.3 (1.90)c*
	ANOVA	P<0.001	P<0.001	P<0.001	P<0.001

Table 3 Relative presence of mineral and degree of crystallinity obtained for the different experimental groups, after Raman spectroscopy analysis. **RPM:** relative presence of mineral (phosphate peak [961 cm^{-1}] and carbonate peak [1070 cm^{-1}] heights) and **FWMH:** degree of crystallinity (full width at half maximum of the phosphate [961 cm^{-1}] and carbonate [1070 cm^{-1}] bands)

		Intertubular Dentin		Intratubular Dentin			
		Phosphate RPM [961cm^{-1}]	Carbonate RPM [1070 cm^{-1}]	Phosphate [961 cm^{-1}]		Carbonate [1070 cm^{-1}]	
				RPM	FWHM	RPM	FWHM
EDTA		50.41	13.57	44.18	22.59	12.13	48.69
After saliva storage	DW	62.44	15.20	54.07	20.01	15.46	34.16
	M	44.55	11.58	33.90	20.10	9.80	30.68
	Zn-M	62.33	18.58	49.39	21.32	13.18	40.37
	B	62.11	13.37	54.16	18.74	13.10	41.84
	Zn-B	97.00	20.94	73.22	19.40	15.04	31.01
	SGB	77.94	13.50	68.88	20.00	13.53	29.75
	NV	87.24	19.20	75.12	21.30	19.15	36.72

		Intertubular Dentin		Intratubular Dentin			
		Phosphate RPM [961cm^{-1}]	Carbonate RPM [1070 cm^{-1}]	Phosphate [961cm^{-1}]		Carbonate [1070cm^{-1}]	
				RPM	FWHM	RPM	FWHM
EDTA		50.41	13.57	44.18	22.59	12.13	48.69
After citric acid	DW	58.20	14.54	34.25	20.01	12.46	61.72
	M	65.72	13.27	39.32	20.68	10.11	58.78
	Zn-M	87.55	19.27	49.66	20.65	12.50	43.61
	B	67.83	15.10	50.82	21.29	11.04	53.20
	Zn-B	92.33	16.16	50.45	20.65	10.78	52.55
	SGB	78.24	16.94	71.96	21.94	15.17	39.30
	NV	81.73	18.11	75.45	22.59	19.24	60.41

Table 4 Mean and standard deviations of dentin permeability after the different treatments and conditions. The values are expressed as (%). The maximum permeability (100%) is assigned to permeability obtained after EDTA treatment. Values with distinct letters in columns and numbers in rows are significantly different after Student-Newman-Keuls multiple comparisons and Student *t* tests respectively ($p<0.05$).

	Dentin permeability (%)	
	After artificial saliva storage for 24 h	After citric acid challenge
DW	64.3 (20.4) a1	97.9 (32.7) A2
M	58.9 (15.3) a1	87.2 (26.7) A2
Zn-M	28.3 (11.2) b1	34.5 (12.3) B1
B	55.3 (16.7) a1	85.7 (27.9) A2
Zn-B	27.8 (12.2) b1	30.5 (10.1) B1
SGB	25.4 (10.3) b1	29.6 (8.9) B1
NV	23.1 (9.6) b1	30.0 (10.5) B1
ANOVA	P<0.001	P<0.001